THE JOURNAL OF BIOLOGICAL CHEMISTRY VOL. 290, NO. 38, pp. 23291–23306, September 18, 2015

Changes in Structural-Mechanical Properties and Degradability of Collagen during Aging-associated Modifications*

Received for publication, February 20, 2015, and in revised from, July 21, 2015 Published, JBC Papers in Press, July 29, 2015, DOI 10.1074/jbc.M115.644310

Preety Panwar[‡§], Guillaume Lamour[¶1], Neil C. W. Mackenzie[†‡§1], Heejae Yang[‖], Frank Ko[‖], Hongbin Li[¶], and Dieter Brömme[‡§2]**

*From the [‡]Department of Oral Biological and Medical Sciences, Faculty of Dentistry, [§]Center for Blood Research, [‖]Department of Mechanical Engineering, and the **Department of Biochemistry and Molecular Biology, Faculty of Medicine, University of British Columbia, Vancouver, British Columbia 6T 1Z3 and the [¶]Department of Chemistry, University of British Columbia, Vancouver, British Columbia V6T 1Z1, Canada*

Background: Extracellular matrix (ECM) alterations during aging contribute to various pathological phenotypes.
Results: Collagen fibrils, fibers, and bone alter their structural integrity and susceptibility toward degradation by cathepsin K when age-modified.
Conclusion: Age-related modifications of collagen affect its biomechanics and proteolytic stability.
Significance: Our research reveals how matrix modifications may increase the risk of ECM disorders.

During aging, changes occur in the collagen network that contribute to various pathological phenotypes in the skeletal, vascular, and pulmonary systems. The aim of this study was to investigate the consequences of age-related modifications on the mechanical stability and *in vitro* proteolytic degradation of type I collagen. Analyzing mouse tail and bovine bone collagen, we found that collagen at both fibril and fiber levels varies in rigidity and Young's modulus due to different physiological changes, which correlate with changes in cathepsin K (CatK)-mediated degradation. A decreased susceptibility to CatK-mediated hydrolysis of fibrillar collagen was observed following mineralization and advanced glycation end product-associated modification. However, aging of bone increased CatK-mediated osteoclastic resorption by ~27%, and negligible resorption was observed when osteoclasts were cultured on mineral-deficient bone. We observed significant differences in the excavations generated by osteoclasts and C-terminal telopeptide release during bone resorption under distinct conditions. Our data indicate that modification of collagen compromises its biomechanical integrity and affects CatK-mediated degradation both in bone and tissue, thus contributing to our understanding of extracellular matrix aging.

Type I collagen is the major extracellular matrix (ECM)[3] protein that provides mechanical stability and structure to various tissues, including tendon, bone, arteries, and skin (1). These macromolecules are self-assembled from collagen triple helices (2). During fibrillogenesis, collagen molecules assemble into fibrils with a characteristic *D*-banding axial periodicity (3–5). Fibrillar rearrangement of collagen provides mechanical characteristics that are crucial for the proper functioning of tissues; indeed, mechanical properties are distributed over distinct hierarchical levels (collagen triple helical molecules, fibrils, and fibers) (6). Alteration in the organization of collagen macromolecules due to aging and other pathological processes may interfere with their realignment and mechanical properties (7–9).

The changes in ECM with increasing age occur due to the reduced synthesis of collagen and unregulated degradation by proteases (10–12). These physiological and pathological modifications lead to dysfunction within a range of tissues, including bone, cartilage, and the cardiovascular and pulmonary systems (13–18). A typical feature of age-related diseases is the ectopic mineralization of ECM. This abnormal mineralization reduces the structural integrity and elasticity of arteries, which impairs cardiovascular function (19, 20). Moreover, alterations in the mechanisms of calcium and phosphorous homeostasis are responsible for both skeletal and vascular disorders (21). Glycation of the matrix is also believed to play a central role in the pathogenesis of aging. In this process, reducing sugars (*e.g.* glucose and ribose) bind to the free amino groups of collagen and go through a series of nonenzymatic reactions to form advanced glycation end products (AGEs). AGEs modify and damage ECM by forming cross-links and contribute to numerous clinical complications associated with aging (22, 23). At the mechanistic level, nonenzymatic glycation leads to the formation of Schiff bases and contributes to a loss in collagen flexibility (24, 25).

* This work was supported by Canadian Institutes of Health Research Grants MOP-8994 and MOP-125866. The authors declare that they have no conflicts of interest with the contents of this article.
We dedicate this work to late Dr. Neil C. W. Mackenzie.
† Deceased.
[1] Both authors contributed equally to this work.
[2] To whom correspondence should be addressed. Tel.: 604-822-1787; Fax: 604-822-7742; E-mail: dbromme@dentistry.ubc.ca.
[3] The abbreviations used are: ECM, extracellular matrix; AGE, advanced glycosylation end product; AFM, atomic force microscopy; BR, bending rigidity; CatK, cathepsin K; CTx, C-terminal telopeptide; EDS, energy-dispersive x-ray spectroscopy; GAG, glycosaminoglycan; OC, osteoclast; PG, proteoglycan; SEM, scanning electron microscopy; TRAP, tartrate-resistant acidic phosphatase; Z, carbobenzoxy; MCA, 4-methylcoumarin amide; BR, bending rigidity; ANOVA, analysis of variance.

Aging-associated modifications have a direct impact on tissue remodeling. Tissue growth factors, proteolytic enzymes, and tissue inhibitors of proteases are regulators of matrix remodeling and tissue development (26, 27). CatK, a cysteine protease, is critically involved in ECM remodeling and responsible for osteoclast-mediated bone resorption, and thus it is integral in skeletal development and maintenance (28). Within the vascular system, it has been shown that CatK is a mechanosensitive protease that is involved in artery remodeling and atherosclerosis, particularly in areas of significant shear stress (29, 30). CatK has been selected as a target for the treatment of osteoporosis and vascular diseases (29, 31, 32). Although CatK and matrix metalloproteinases have been studied in the context of degenerative disorders of the ECM (29, 32–34), significantly less is known about the effects of pathophysiological modifications of collagen on its degradation by CatK and whether matrix glycation and mineralization lead to increased degradation or vice versa.

In this study, we evaluated the structural and mechanical changes that occur in the collagenous components following various modifications and how CatK responds under these conditions. To describe the consequences of mineralization, accumulation of AGEs, and the depletion of glycosaminoglycans (GAGs) on collagen macromolecules, we analyzed their *in vitro* CatK-mediated degradation. To model pathological processes in the skeletal system, we studied aging-related modification of bone matrix through osteoclast-mediated bone resorption.

Experimental Procedures

Materials—EDTA, dithiothreitol (DTT), dimethylmethylene blue, ribose, methylglyoxal, and chondroitinase ABC were obtained from Sigma. 100 mM sodium acetate buffer, pH 5.5, containing 2.5 mM EDTA and 2.5 mM DTT was used for collagen degradation assay. Z-Phe-Arg-MCA was obtained from Bachem (Weil am Rhein, Germany). Cellu-Sep® cellulose dialysis tubing (molecular weight cutoff 12,000–14,000) was purchased from Membrane Filtration Products Inc. (Seguin, TX). Calcium and phosphate concentrations were determined by colorimetric assay using calcium and phosphate assay kit (Abcam Inc., Toronto, Ontario, Canada). CTx-I detection kit was purchased from Antibodies Online Inc. (Atlanta, GA). Tartrate-resistant acid phosphatase (TRAP) staining kit was obtained from Sigma. Receptor activator of nuclear factor κB ligand and macrophage colony-stimulating factor were purchased from R&D Systems (Minneapolis, MN). CatK was expressed in *Pichia pastoris* and purified as described previously (35).

Reconstitution of Collagen Fibrils—Type I collagen fibers were extracted from 3-month-old C57BL/6 mice tails, swollen in acetic acid (0.05 M) overnight at 4 °C, and stirred at 500 rpm for 2 days. The resulting collagen suspension was centrifuged for 15 min at 8,000 × *g*, and the pellet was lyophilized. Fibrils without any modification were considered as native. Fibrils were mineralized using simulated body fluid (SBF), pH 7.4, as described previously by Kokubo and Takadama (36). The concentrations of Ca^{2+} used for the mineralization experiments were 1.5, 2.5, and 4.5 mM and for HPO_4^{2-} were 0.5, 1.0, and 2.0 mM. They are designated as low, intermediate, and high degree of mineralization. Ca^{2+} (2.5 mM) and HPO_4^{2-} (1.0 mM) ion concentrations are equal or close to those in blood plasma (37). Sodium azide (2.5 mM) was added to avoid bacterial growth. For mineralization, the precipitated fibril pellet was suspended in SBF medium and incubated for 5 days at 4 °C. AGE modification of collagen fibrils and fibers was obtained after incubation with 3, 6, and 15 mM ribose and 2, 4, and 10 mM methylglyoxal in phosphate buffered saline (PBS), pH 7.4, at 4 °C for 5 and 15 days, respectively. Removal of GAGs from collagen fibrils was carried out by overnight digestion with chondroitinase ABC (100 milliunits) at 28 °C in 10 mM Tris-HCl, 25 mM sodium acetate, pH 7.4. Native and GAG-depleted collagen fibrils were incubated with PBS for 5 days at 4 °C. During incubation, all categories of collagen fibrils were constantly stirred at 50 rpm. The resulting fibrils were dialyzed and filtered and used for AFM analysis after collagen quantification.

Analysis of Collagen Fibril Modification—A commercially available colorimetric method was used to determine the concentrations of calcium and inorganic phosphate (P_i) in mineralized and unmineralized fibrils. AGE content was determined based on the fluorescence assay described by Monnier *et al.* (38). The AGE content was measured fluorometrically at the excitation and emission wavelengths of 370 and 440 nm, respectively, and calculated as fluorescence units/mg collagen. Total collagen concentration was measured using hydroxyproline assay for all categories of fibrils (Sigma). GAG concentration was determined spectrophotometrically using dimethylmethylene blue assay (39).

Structural and Mechanical Analysis of Fibrils by Atomic Force Microscopy—Fibrils were imaged using atomic force microscopy (AFM; Cypher™, Asylum Research, Santa Barbara, CA) to derive structural and mechanical parameters such as persistence length and Young's modulus of elasticity. AFM images were collected for four different types of collagen fibrils as follows: native, mineralized, AGE-modified, and GAG-depleted fibrils. Collagen fibrils (10 μl) of 1 μg/ml concentration were deposited on freshly cleaved mica for 15 min, rinsed three times with deionized water, and air-dried. Imaging was done using the air tapping mode, and images were acquired at a 3-Hz scanning rate using silicon tips (AC160TS from Asylum Research) with a nominal spring constant of 42 newtons/m. AFM topographic data were acquired for ~50 fibrils of each type. Single fibrils were analyzed to determine the persistence length from which the stiffness is derived. AFM heights and statistical analysis of variations in fibril shape were used to determine the mechanical properties of these structures as described in previous studies for protein fibrils (40, 41). The contour of fibrils was fitted to parametric splines, and the persistence length (P_L) was determined using a worm-like chain model for semi-flexible polymers (42). Scaling exponent analysis of the end-to-end distance as a function of the inner contour length (43) suggested that the fibrils equilibrated on the mica surface; therefore, a worm-like chain model considering fluctuations in two dimensions was used. The Young's modulus of elasticity (Y) was derived by using $Y = BR/I$, where BR is the bending rigidity ($BR = P_L \cdot k_B \cdot T$, with k_B the Boltzmann constant and T the temperature), and I is the second moment of area. A

cylindrical cross-section was assumed to estimate I according to $I = \pi \cdot h^4/64$, where h is the fibril height.

Modification of Collagen Fibers—Mouse tail collagen fibers were mineralized using simulated body fluid, pH 7.4 (36), at 20 °C for 15 days. For control experiments, fibers (native) were incubated with PBS, pH 7.4. AGE-related modification of collagen fibers was performed as described above by incubating fibers with ribose and methylglyoxal in PBS, pH 7.4, at 4 °C for 15 days. Native collagen fibers were prepared similarly without the AGE precursors. To obtain GAG-depleted fibers, collagen-bound glycosaminoglycans were removed by repeated overnight treatment with chondroitinase ABC (200 milliunits) as described above. Modified fibers were dialyzed against distilled water for 1 day.

Ultrastructural and Microchemical Analysis of Collagen Fibers—Scanning electron microscopy (SEM) was used to determine structural changes of the collagen fibers due to modifications and CatK digestion. For SEM, samples were prepared as described previously, mounted on carbon adhesive, coated with gold/palladium, and subsequently imaged using a Helios NanoLab^{TM} 650 microscope (FEI, Hillsboro, OR) (44). Microchemical analysis of elements for both mineralized and native (unmineralized) collagen fibers was done using SEM equipped with energy-dispersive x-ray spectroscopy (EDS) at an accelerating voltage of 8 kV and beam current of 6.4 nA. Collagen specimens were mounted on the metal stub with adhesive tape and coated with carbon using a Leica EM MED020 coating system (Leica Microsystems Inc., Concord, Ontario, Canada), and the EDS spectrum and maps were collected to identify the location and amount of calcium and phosphorus. Native (control) and modified fibers were homogenized for 24 h at 4 °C and centrifuged at 13,000 × *g* for 30 min. Concentration of AGEs and GAGs were determined as described above.

Micro-tensile Testing of Collagen Fibers—Collagen fibers were tested for their mechanical stability before and after CatK digestion. SEM and optical microscopy were used for diameter measurements. Tensile strength of control ($n = 25$) and CatK-digested fibers ($n = 25$) was measured by a KES-G1 tensile testing machine (Kato Tech Co., Ltd., Kyoto, Japan). Tensile tests were performed with a 50-newton capacity load cell, and a gauge length of 10 mm was selected. Both control and digested fibers were stretched in a uniaxial direction until failure at a cross-head speed of 0.6 mm/min was observed (44, 45).

CatK-mediated Degradation of Collagen Fibrils and Fibers—Native, mineralized, AGE-modified, and GAG-depleted collagen fibers (1 mg) and fibrils (1 mg/ml) were digested with 3 μM and 400 nM CatK, respectively, in 100 mM sodium acetate buffer containing 2.5 mM DTT and EDTA, pH 5.5, for different time points at 28 °C. The CatK reaction was terminated with 10 μM E-64, and supernatants for SDS-PAGE analysis were collected after 20 min of centrifugation. SDS-PAGE analysis was performed in 9% Tris/glycine gels, stained by Coomassie Brilliant Blue R-250, and quantified by SYNGENE, Bioimaging system. To compare the degradation level of different categories of fibers, the content of C-terminal telopeptide (CTx) of type I collagen was measured using an immunosorbent assay. Residual CatK activity was measured at each time point using the synthetic peptide substrate, Z-Phe-Arg-MCA. Binding assay was performed to determine the effects of collagen modifications on collagen-CatK binding. For binding experiments, native and modified fibers were incubated separately with CatK, and the residual activity of CatK in digestion medium was measured using Z-Phe-Arg-MCA as the substrate. The CatK concentration in digestion medium correlates to the amount of unbound protein.

Structural and Mechanical Characterization of Bone—Bovine cortical bones from young (~1 year), mature (~5 years), and aged (<9 years) animals were obtained from the slaughterhouse. A similar area of each femur bone was used for bone slicing. Bone slices were demineralized by incubating with 0.1 M EDTA at 4 °C for 10 days. For the removal of GAGs, demineralized bone slices were treated twice with chondroitinase ABC (200 milliunits) at 28 °C overnight in 10 mM Tris-HCl, 25 mM sodium acetate, pH 7.4. Here, we designated collagen of mature bones as native collagen. Topographical analysis of the bone surface was determined by SEM. Bone slices (500 μm thick, 10 mm long, and 1.75 mm wide, $n = 15$, each condition) were prepared from a similar region and used for mechanical testing at a displacement rate of 15 mm/min using 50 newton cells.

Resorption of Bone Matrix by Osteoclasts (OCs)—We cultivated human OCs on native, demineralized, young, aged, and GAG-depleted bone slices to compare the resorption level after the various modifications. OCs were generated from mononuclear cells isolated from human bone marrow purchased from Lonza (Walkersville, MD). Mononuclear cells were cultured in α-minimum essential media supplemented with 10% FBS, 1% penicillin/streptomycin, 2 mM L-glutamate, and 25 ng each of receptor activator of nuclear factor κB ligand and macrophage colony-stimulating factor as described previously (46). Differentiated OCs at a density of 50,000 cells were seeded on each bovine bone slice and incubated for 72 h at 5% CO_2 and 37 °C. The resorption features were analyzed by staining bone discs with toluidine blue, and the total number of osteoclasts cells was determined after TRAP staining. Cells were fixed in 4% formaldehyde and were subsequently stained for TRAP activity (Sigma). Cells with more than two nuclei were counted to determine the total number of OCs per bone slice at each experimental condition. Images were acquired using a Nikon Eclipse LV100 microscope. Collagenolysis by OCs was determined by measuring the release of the CTx marker.

Statistical Analysis—All data are means ± S.D. Statistical significance was determined by ANOVA.

Results

In this study, we have exploited biochemical and biomechanical methods to simulate and characterize pathophysiological modifications of collagen fibrils and fibers during aging.

Mechanics of Fibrils after Aging-related Modifications—Here, we analyzed low level mineralized and AGE-modified fibrils, which are more physiologically relevant. To determine how collagen fibers confer mechanical strength to tissues, an understanding of the mechanical properties at a lower hierarchical level is essential. *In vitro* modification of fibrils exposed

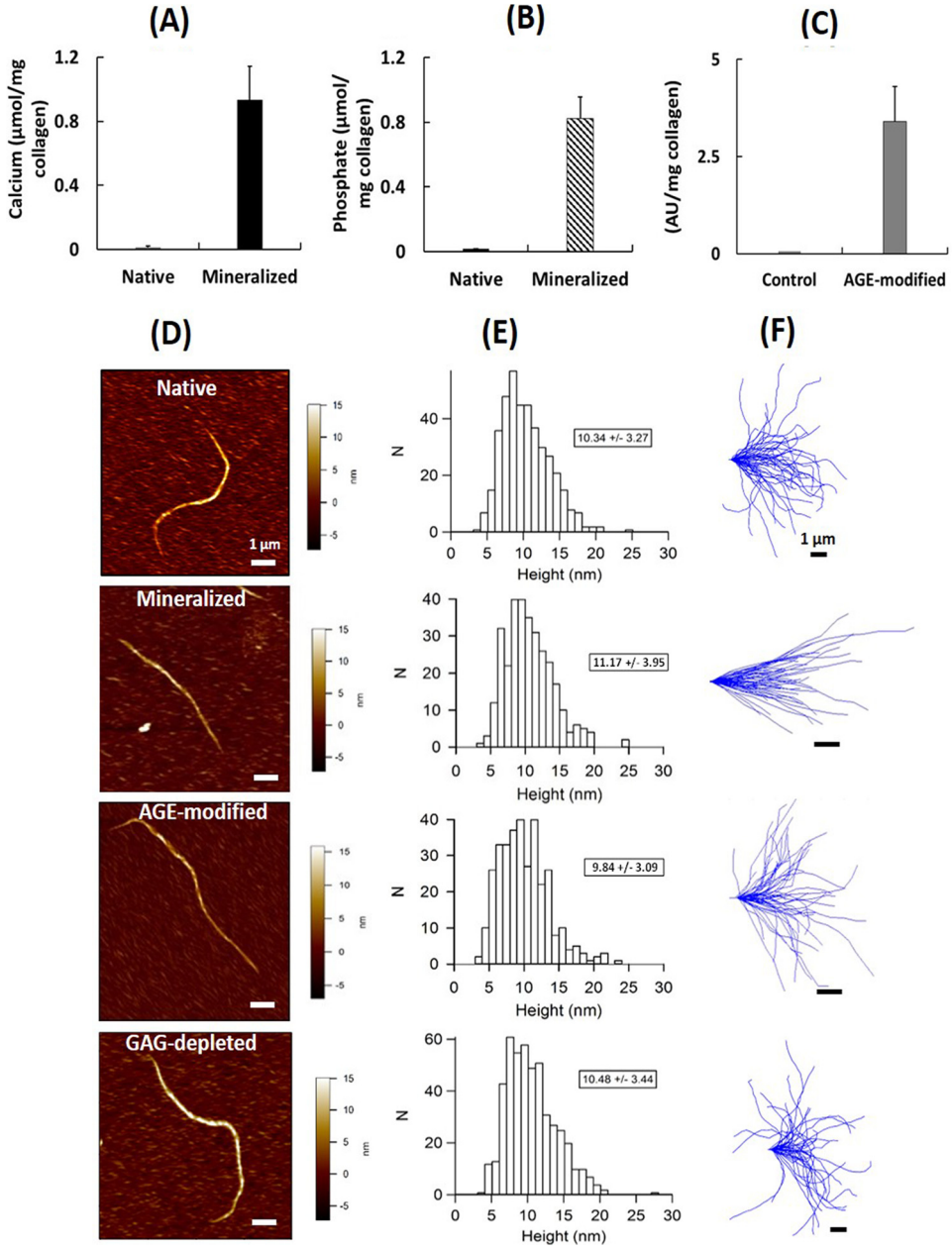

FIGURE 1. Calcium (*A*) and phosphate (*B*) concentrations in native and mineralized fibrils are shown. *C*, accumulation of AGEs is seen in AGE-modified fibrils. *D–F*, AFM analysis of native and modified collagen fibrils. *D*, AFM topographic data of individual fibrils; *E*, heights measured from 50 fibrils with 10–15 height measurements per fibril (box value, the average heights obtained from Gaussian fit expressed in SEM ± S.D.); and *F*, contours of 50 fibrils each of the native, mineralized, AGE-modified, and GAG-depleted group (sequence, *top to bottom*). The contours of fibrils have been aligned according to their initial tangents to facilitate the visualization of flexural rigidities of the fibrils. These are derived from shape fluctuation analysis (see under "Experimental Procedures").

to minerals and AGEs are shown in Fig. 1, *A–C*. Using AFM, we observed structural variations among native and modified fibrils (Fig. 1, *D–F*). Several polymer-based studies have described the shape fluctuations of biological filaments to determine their mechanical properties (47, 48). Alterations in shape and filament sizes were extracted from AFM images to derive the persistence length (P_L), the BR, and the Young's modulus of native and modified collagen fibrils. P_L and BR (= $P_L \cdot k_B \cdot T$) indicate the elastic properties of the fibrils. The higher the P_L value is, the stiffer the fibril. P_L and contour lengths of native and modified fibrils are summarized in Table 1. Our results reveal that the bending rigidities of the collagen fibrils vary with mineral content, AGE modification, and GAG depletion. We calculated the cross-sectional moments of inertia (*I*) for each type of fibril from their average heights in the AFM measurements, and analysis of *I versus* BR showed that each of the fibril types can be characterized by a distinct Young's mod-

TABLE 1
Mechanical properties of native and modified collagen fibrils

Fibril treatment	Persistence length (P_L)	Young's modulus	Contour length
	µm	*MPa*	*µm*
Native	3.5 ± 0.5	11–95	6.9 ± 2.2
Mineralized	68 ± 12	97–1420	3.6 ± 1.8
AGE-modified	8.0 ± 1.8	23–182	5.1 ± 2.1
GAG-depleted	1.3 ± 0.4	3–36	5.9 ± 2.3

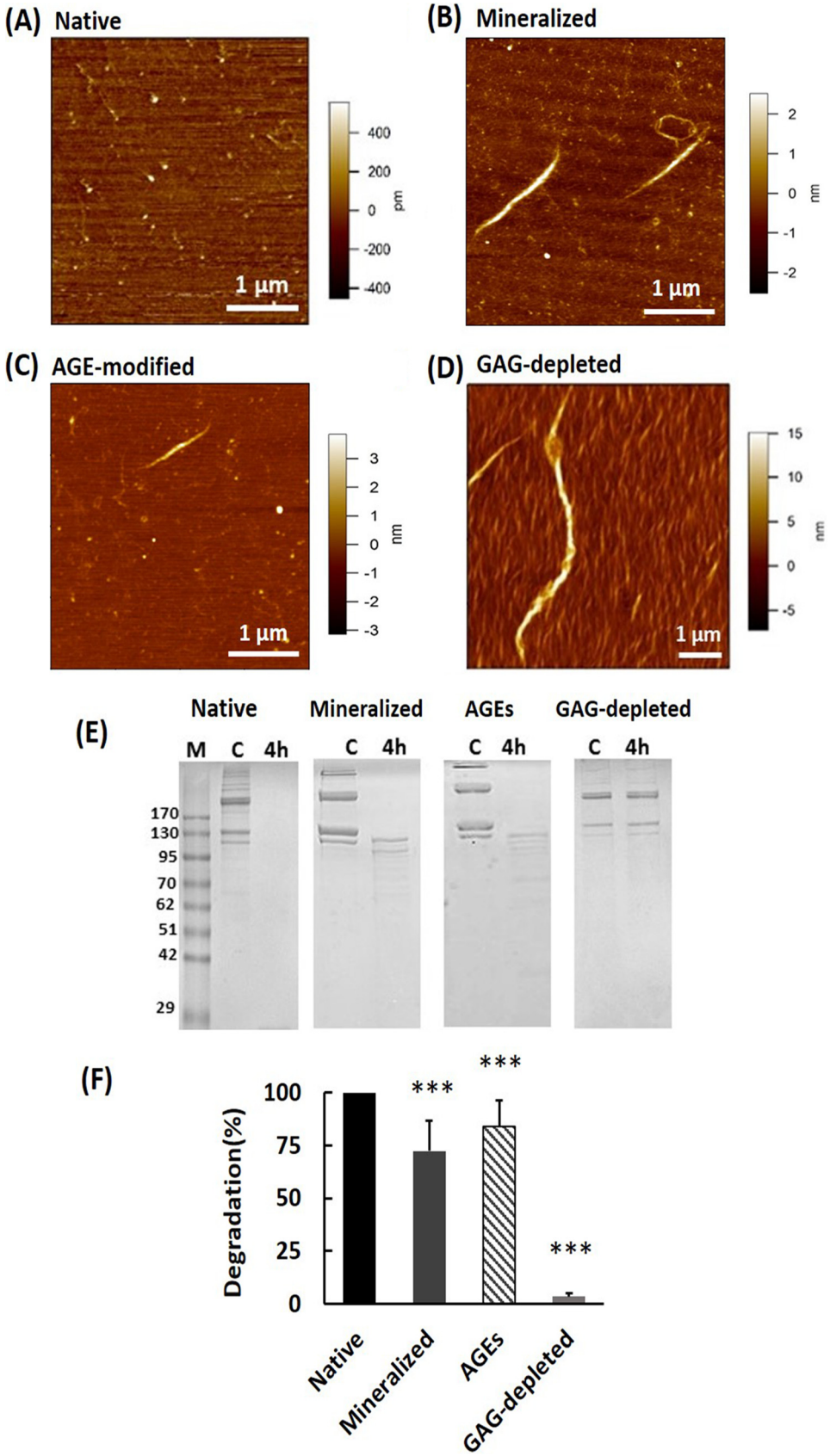

FIGURE 2. **AFM analysis of collagen fibrils following degradation by CatK.** *A–D,* AFM images of CatK-digested collagen at 4 h incubation of native (*A*), mineralized (*B*), AGE-modified (*C*), and GAG-depleted fibrils (*D*). *E,* SDS-PAGE analysis shows the complete degradation of native fibrils, whereas mineralized and AGE-modified fibrils show less degradation. *F,* quantification of the degradation of fibrils. *M,* protein marker; *C,* control collagen unmodified or modified. Statistical significance was tested with ANOVA. ***, $p < 0.001$ *versus* native fibrils.

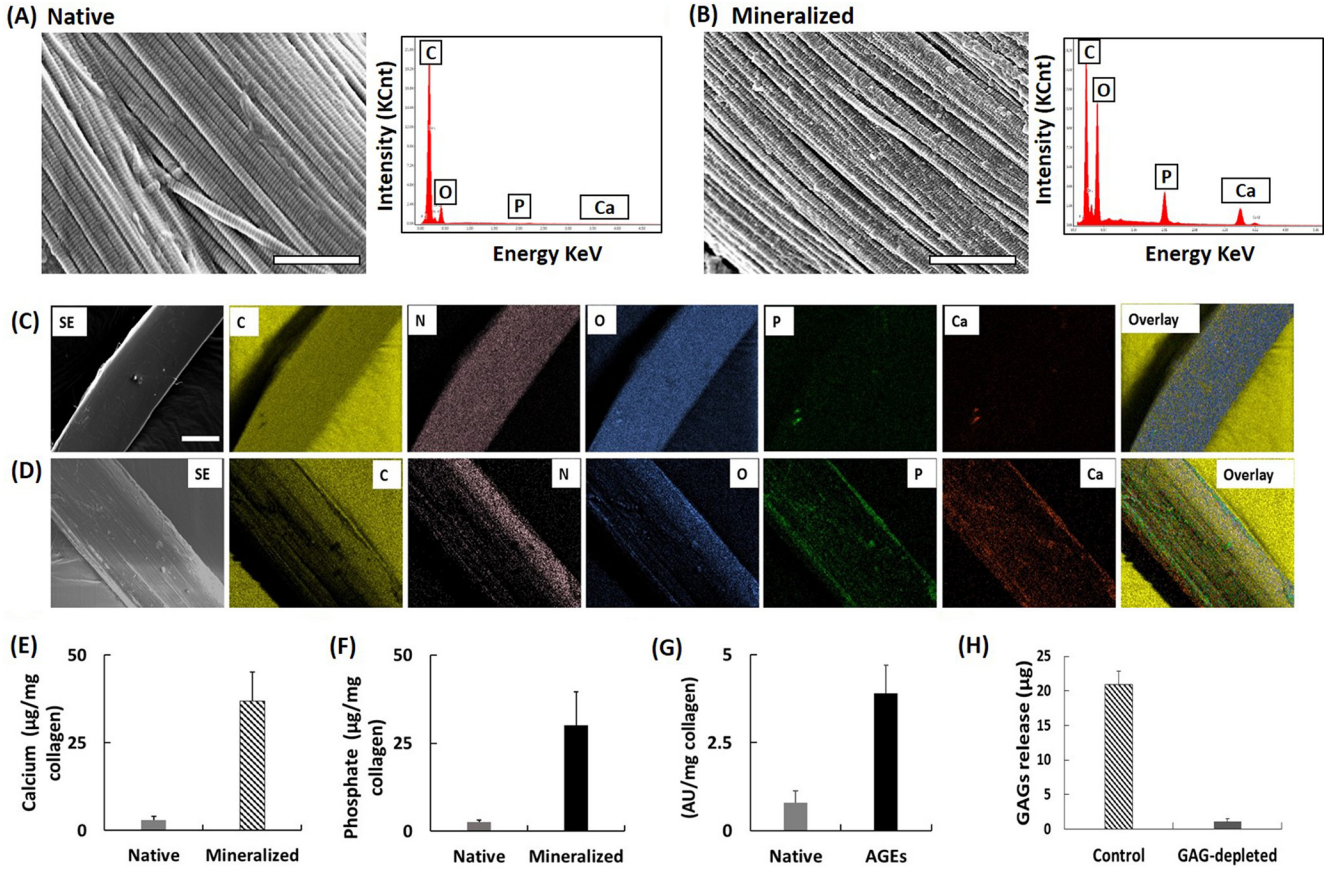

FIGURE 3. *A–D,* S. E. micrographs of the surface of native (*A*) and mineralized (*B*) fibers and the corresponding EDS spectra. *Scale bar,* 2 μm. EDS spectra were collected using point analysis. Similar spectra were obtained at multiple sites on the micrographs, confirming the homogeneous binding of elements all over the surface. EDS mapping of native (*C*) and mineralized (*D*) fibers showing secondary electron (*SE*) images and digital images of the elements carbon, oxygen, nitrogen, calcium, and phosphorus and their overlay. *E* and *F,* comparison of calcium (*E*) and phosphate (*F*) concentrations in native and mineralized fibers. The accumulation of AGEs is clearly seen in AGE-modified fibers and is presented in arbitrary fluorescence units (*AU*) per mg of collagen (*G*). Effect of chondroitinase ABC on collagen fibers and release of GAGs is shown (*H*). *Scale bar,* 25 μm.

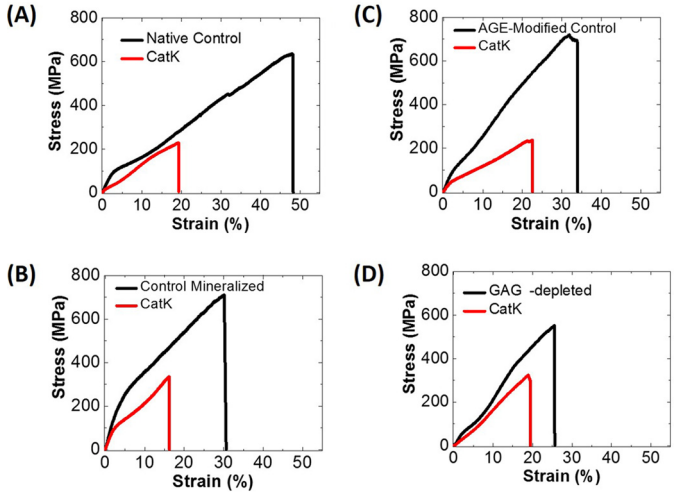

FIGURE 4. **Mechanical properties of native and modified collagen fibers.** *A–D,* stress-strain plots for native (*A*), mineralized (*B*), AGE-modified (*C*), and GAG-depleted fibers (*D*). *Plots* represent the comparison of stress-strain between undigested ($n = 25$) and CatK-digested fibers ($n = 25$). Fibers were digested with CatK for 2 h, and stress-strain curves were obtained from the displacement of 0.6 mm/min in dry conditions.

ulus of elasticity of native ($Y = 11–95$ MPa), GAG-depleted ($Y = 3–36$ MPa), AGE-modified ($Y = 23–182$ MPa), and mineralized fibrils ($Y = 97–1420$ MPa). They clearly reflect differences in material properties from one fibril type to another. It is interesting to note that the changes in intrinsic stiffness originated from differences in persistence length only, because the AFM heights of each fibril type were quite similar. Both AGE modification and mineralization of fibrils severely altered their intrinsic properties and increased their Young's modulus significantly.

CatK-mediated Degradation of Native and Modified Collagen Fibrils—As described above, the mechanics of fibrils vary after modification. Here, we observed the effect of CatK on these modified nanostructures. At the microscopic level, native fibrils were completely denatured and degraded by CatK (Fig. 2*A*); however, GAG-depleted fibrils remained unchanged after exposure to the same enzyme concentration (Fig. 2*D*). Conversely, AGE-modified and mineralized fibrils displayed degradation products of different heights, likely corresponding to different states of fibril degradation (Fig. 2, *B* and *C*). SDS-PAGE analysis of collagen α-fragments revealed that native fibrils were completely degraded by CatK in 4 h, but for AGE-modified and mineralized fibrils, remnants of α-chains remained, and no degradation was detected for GAG-depleted collagen fibrils (Fig. 2, *E* and *F*). Residual activities of CatK were identical at different incubation time points of digestion for native and modified fibrils (data not shown).

TABLE 2
Mechanical properties of native and modified collagen fibers before and after CatK digestion
Average diameters of collagen fibers were calculated from multiple spots on the same fiber. MPa is megapascal and GPa is gigapascal.

	Diameter	Strength	Young's modulus	Stress at break	Strain at break
	μm	*N*	*GPa*	*MPa*	*%*
Fiber treatment					
Native	59.00 ± 14.81	2.02 ± 0.45	3.03 ± 0.40	605 ± 100	43 ± 6.9
Mineralized	67.82 ± 13.74	2.81 ± 0.34	3.74 ± 0.25	713 ± 89	29 ± 4.2
AGE-modified	74.64 ± 12.71	2.47 ± 0.56	3.48 ± 0.27	688 ± 75	36 ± 4.8
GAG-depleted	75.70 ± 14.31	1.86 ± 0.45	2.46 ± 0.35	450 ± 97	23 ± 4.5
CatK-digested					
Native	83.00 ± 15.59	1.32 ± 0.31	1.81 ± 0.28	230 ± 55	21 ± 5.2
Mineralized	80.21 ± 14.43	1.78 ± 0.62	2.35 ± 0.44	386 ± 52	16 ± 2.8
AGE-modified	85.38 ± 10.72	1.63 ± 0.40	2.04 ± 0.18	341 ± 47	17 ± 5.4
GAG-depleted	89.50 ± 11.12	1.46 ± 0.63	1.70 ± 0.30	350 ± 84	18 ± 4.4

Characterization of Native and Modified Collagen Fibers—We analyzed low level mineralized and AGE-modified fibers. Topographical observations of mineralized fibers showed the deposition of dense structures on the surface of collagen fibers compared with native (unmineralized) fibers (Fig. 3, *A* and *B*). EDS spectrum analysis verified the presence of calcium and phosphorus on the mineralized fibers. EDS mapping images of carbon, oxygen, nitrogen, calcium, and phosphorus and their overlay clearly revealed higher intensities of Ca and P in mineralized fibers (Fig. 3*D*) when compared with unmineralized samples (Fig. 3*C*), which was further confirmed by colorimetric analysis (Fig. 3, *E* and *F*). Fig. 3*G* shows the degree of accumulation of AGEs in control and AGE-modified fibers, indicating their acquired modifications. Spectrophotometric quantification of GAGs in GAG-depleted fiber revealed the removal of polysaccharide chains after chondroitinase ABC treatment (Fig. 3*H*).

We also performed uniaxial tensile tests on native, mineralized, AGE-modified, and deglycosylated collagen fibers. An increase in the modulus explains the reduction in extensibility or elasticity for the mineralized and AGE-modified fibers. The maximal stress applied on the collagen fibers prior to their breaking was the highest for mineralized fibers followed by AGE-modified and native and lowest for GAG-depleted fibers. These results revealed that mineralized fibers are extremely stiff and have the lowest failure strain, whereas unmineralized fibers exhibit maximum extensibility under comparative stress. As a result of CatK digestion, the stress-strain behavior of the collagen fibers was altered and exhibited low levels of breaking stress and breaking elongation as shown in Fig. 4. Mechanical characteristics of native and modified fibers are given in Table 2.

Ability of CatK to Degrade Collagen Fibers after Modification—Microscopic analysis of native collagen fibers revealed the progressive unraveling of the fibrillar structure and their complete degradation (Fig. 5, *A, E,* and *I*) (44). In contrast to native fibers, mineralized fibers were not completely degraded by CatK (Fig. 5, *B, F,* and *J*). Structural and protein electrophoretic analysis of degradation products confirmed the slow degradation of AGE-modified fibers (Fig. 5, *C, G,* and *K*) and negligible degradation of GAG-deficient fibers by CatK (Fig. 5, *D, H,* and *L*). In addition, we also observed the combined effect of AGEs and mineralization, which limited the unfolding and degradation of collagen fibers by CatK (data not shown). Degradation assays show mineralized and AGE-modified collagen with a slower rate of digestion when compared with native collagen fibers, and GAG-depleted collagen is almost completely protected from degradation (Fig. 6*A*). However, CatK-mediated degradation can be reinstated by addition of chondroitin sulfate to the GAG-depleted collagen fibers (Fig. 7). As a marker of CatK-mediated collagen degradation, we analyzed the release of CTx. The overall CTx release from AGE-modified fibers was similar to that of native fibers but comparatively less during the initial phase of degradation, which confirms their slower digestion (Fig. 6*B*). The different rates of degradation of the modified collagen fibers were not related to secondary effects on CatK activity and stability as the residual activity of the protease toward the synthetic substrate, Z-Phe-Arg-MCA, was similar at different time points during the incubation (data not shown). To test whether CatK-collagen binding was affected, we analyzed the residual activity of unbound CatK using Z-Phe-Arg-MCA method. Compared with 95% binding of CatK to native collagen, its binding was reduced to 55, 40, and 82% in mineralized, AGE-modified, and GAG-depleted fibers, respectively.

Effect of Increasing Concentrations of Minerals and AGEs on Collagen Fibers and Fibrils—We compared the effect of low, intermediate, and high level mineralization and AGE modification on CatK-mediated degradation and mechanical stability of collagen fibrils and fibers. The degree of collagen mineralization was determined by EDS and biochemical analysis (Fig. 8). We demonstrated that high level mineralized fibers and fibrils allowed an ~55% CatK-mediated degradation when compared with ~75% degradation at low degree mineralization (Fig. 9*A*). Stiffness of collagen fibers increased with increasing levels of mineral and AGE modifications (Tables 3 and 4). Similarly, AFM studies show that mineralized fibrils were stiffer than native fibrils. When we compared different degrees of mineralization on the mechanical properties of fibrils, we observed that the persistence length (P_L) and Young's modulus of fibrils slightly change with increasing mineral content. AGEs reduced CatK-mediated collagen degradation by ~20% and increased collagen stiffness. Excessively increased levels of AGE-mediated collagen modifications did not further affect the collagen fiber and fibril degradation (Fig. 9*B*).

Consequences of Modifications on the Bone Matrix—The surface topography of native and physiologically challenged bones was visualized by SEM, and their representative images are

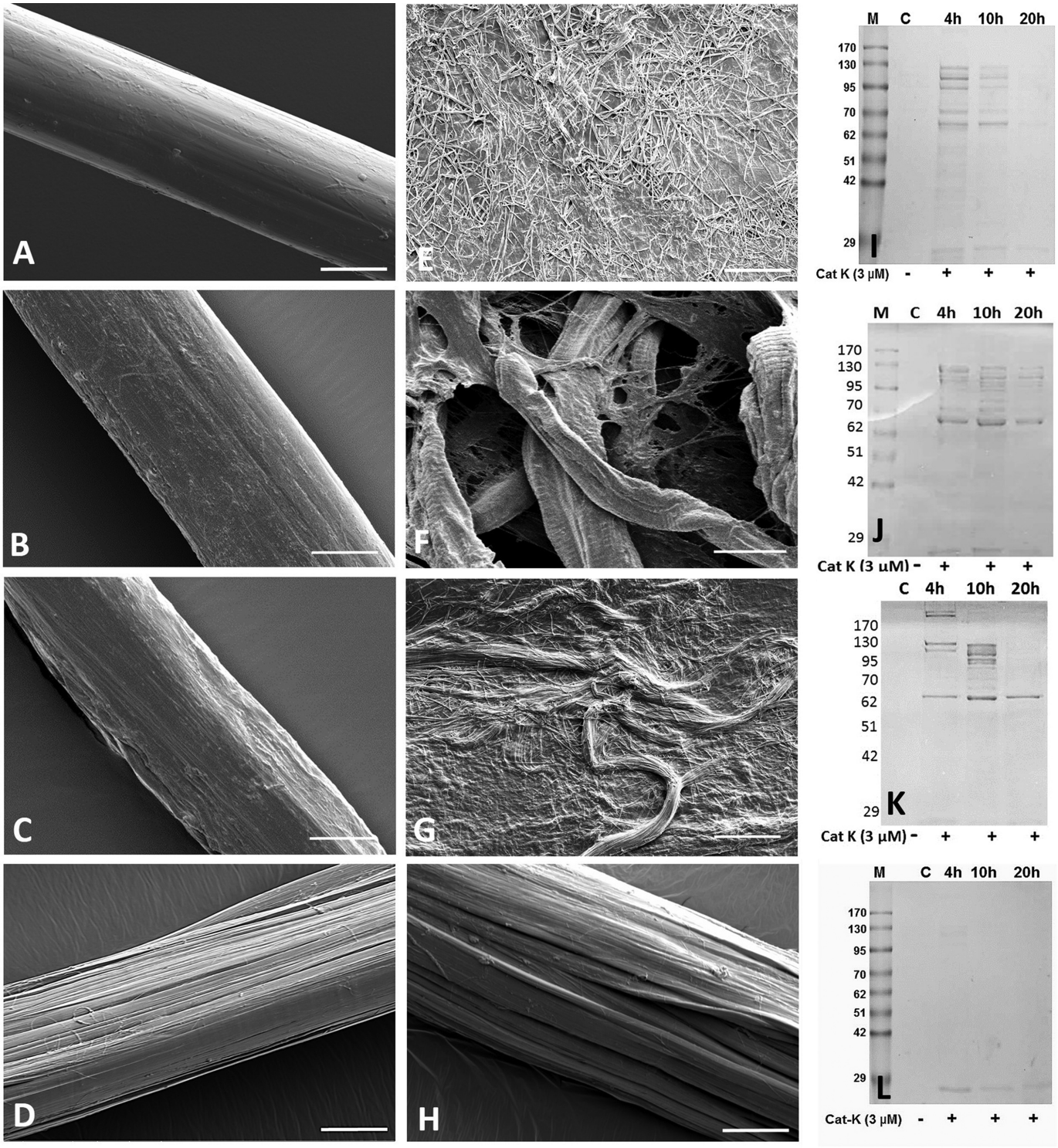

FIGURE 5. **CatK-mediated degradation of native and modified collagen fibers.** SEM images of modified control collagen fibers (*left column*), fibers digested with CatK for 12 h (*middle column*), and SDS-PAGE analysis of degradation fragments after incubation with CatK at different time points up to 20 h (*right column*). SEM micrographs of native (*A*), mineralized (*B*), AGE-modified (*C*), and GAG-depleted (*D*) collagen fibers depict structural changes. Degradation of collagen fibers with 3 μM CatK at pH 5.5 and 28 °C displayed a more extensive degradation of native fibers (*E*) when compared with mineralized (*F*) and AGE-modified fibers (*G*). No CatK-mediated degradation was observed for GAG-depleted fibers (*H*). *Scale bars* represent 25 μm. *I–L, M* stands for molecular weight and *C* for control without CatK. SDS-PAGE analyses of degradation products of mineralized (*J*) and AGE-modified (*K*) fibers show comparatively less degradation than native fibers (*I*) and no degradation of GAG-depleted fibers (*L*) at different time points.

shown in Fig. 10*A*. Tensile testing of bone specimens indicated significant variations in modulus of physiologically challenged compared with native bones. The tensile strength and Young's modulus of mineralized/native bone slices were significantly higher than those of demineralized bone slices. However, tensile testing results of younger and native bones showed comparatively higher breaking load and modulus when compared with aged bone slices (Table 5).

Effect of Bone Modification and Aging on OC-mediated Resorption—We examined the resorptive potential of OCs cultured on bone slices of different ages and modified bone matrix.

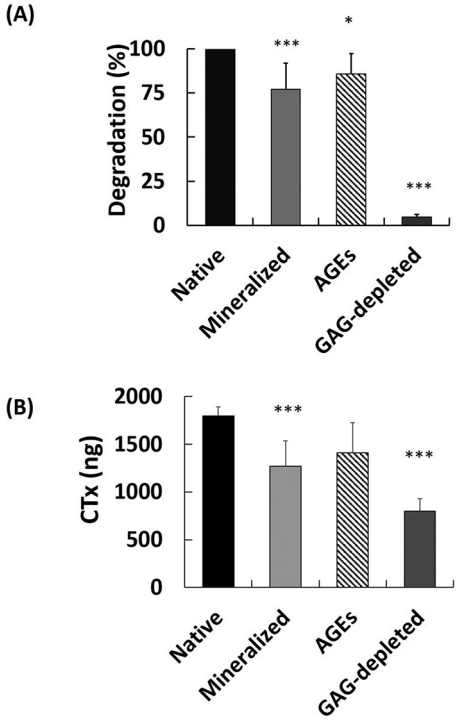

FIGURE 6. **Quantitative analysis of collagen degradation products.** *A,* degradation of native, mineralized, AGE-modified, and GAG-depleted fibers after 20 h of digestion with CatK. Statistical significance was tested with ANOVA. ***, $p < 0.001$; *, $p < 0.05$ *versus* native fibers. *B,* release of C-terminal telopeptide of type I collagen (CTx) from native, mineralized, AGE-modified, and GAG-depleted insoluble collagen fibers by CatK after 20 h. Native and physiologically modified fibers (1 mg) were digested with 3 μM CatK at pH 5.5 and 28 °C, and α-chains and CTx were measured in the supernatant. Statistical significance was tested with ANOVA. ***, $p < 0.001$ *versus* native fibers.

Demineralized and young bones showed a lower number of $TRAP^+$-multinucleated cells attached to the surface when compared with mineralized and aged bones, respectively (Fig. 10, *B* and *D*). Although most of these conditions showed some differences in OC adhesion on the bone surface, the major differences were seen in the type of excavations generated by OCs and resorbed bone surface. Mature bone displayed resorption lacunae in the form of long deep trenches, whereas negligible imprints of OC activity were observed in demineralized bone. The resorption cavities in the matrix of young bones were similar to middle-aged bone; however, greater numbers of long trenches were observed in aged bone (Fig. 10*C*). Demineralization of bone caused a significant reduction in bone resorption by OCs as assessed by the total resorption area, and an overall less resorbed surface was observed in young bones compared with aged bones (Fig. 10*E*). Removal of GAGs from demineralized bone slices showed reduced bone resorption by OCs and was comparably low as for demineralized bone. The resorption activity of OCs on different categories of bone slices was measured by CTx release in the medium (Fig. 10*F*). We found that CTx release was higher from mineralized when compared with demineralized bones. Similarly, a significant increase in CTx release was observed in aged compared with young bones.

Discussion

Increased cross-linking and accumulation of minerals within the ECM and soft tissues is a natural response to physiological stress and aging. These modifications lead to significant changes in structural and mechanical properties of ECM proteins and affect the normal remodeling of tissue by interfering with proteolytic degradation. A number of studies have shown the deposition of brushite and hydroxyapatite in soft tissues, which occurs by passive precipitation of minerals during numerous pathological conditions (49, 50). Atherosclerotic

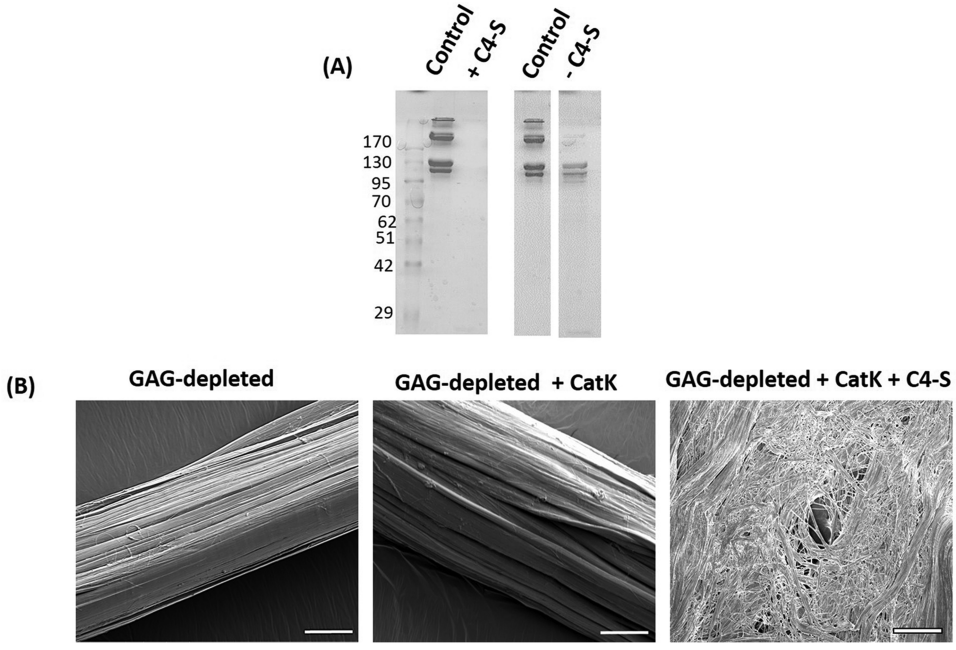

FIGURE 7. *A,* degradation of collagen fibrils with and without chondroitin 4-sulfate (*C4-S*). *B,* SEM images of GAG-depleted collagen fibers and their degradation by CatK. SEM micrographs show the effect of rescuing CatK-mediated degradation by adding chondroitin 4-sulfate to GAG-depleted collagen fibers. *Scale bar,* 25 μm.

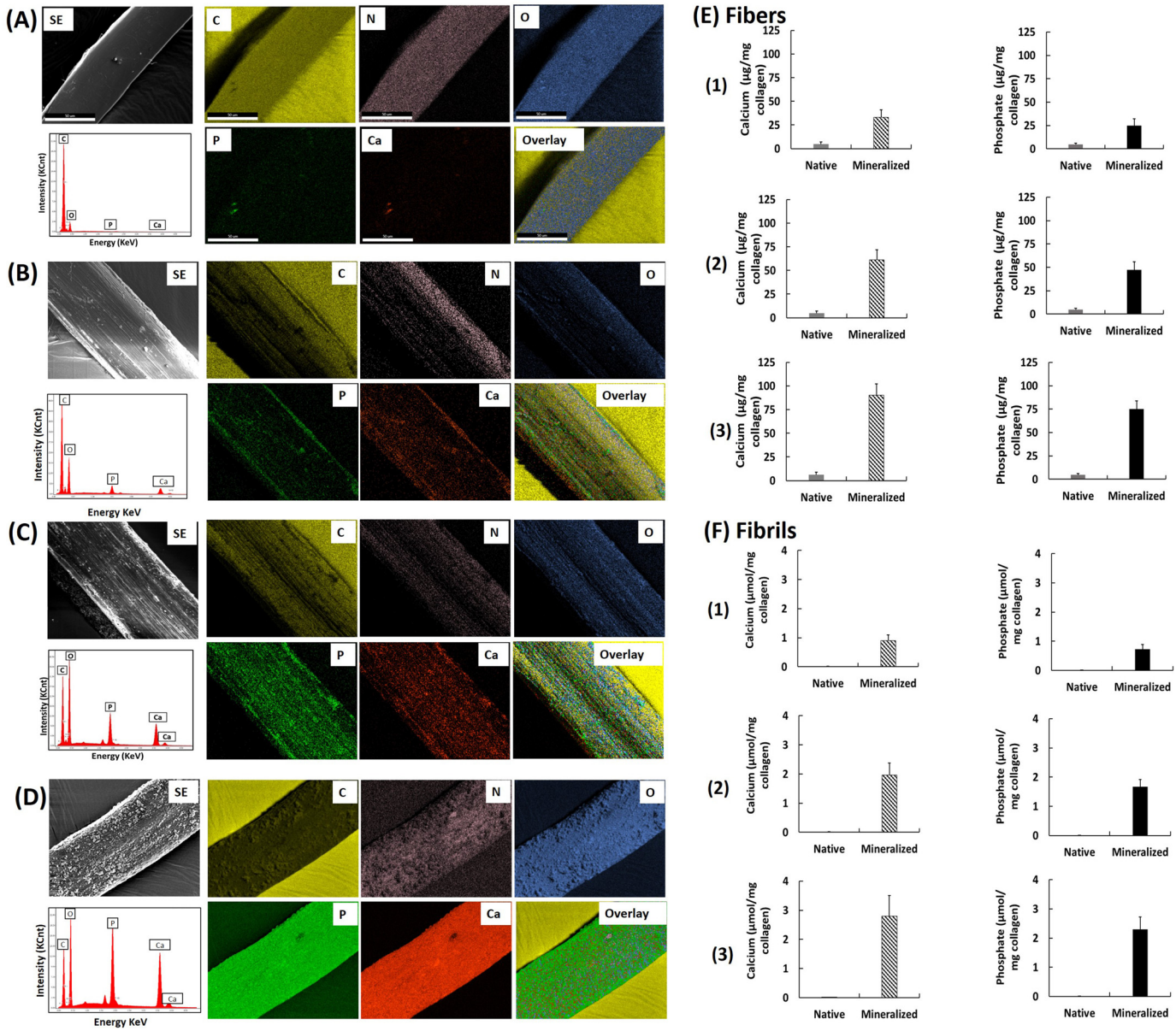

FIGURE 8. EDS mapping of native (unmineralized) (*A*), weakly mineralized (*B*), intermediately mineralized (*C*), and highly mineralized (*D*) collagen fibers showing secondary electron (*SE*) images and digital images of the elements carbon, oxygen, nitrogen, calcium, their overlay, and EDS spectra. The overlay images of mineralized fibers show denser material in *green/red* and the less dense material on the surface of less mineralized collagen fibers. *Scale bar,* 50 μm. *E,* comparison of calcium and phosphate concentrations in native and mineralized fibers as follows: *panel 1,* low; *panel 2,* intermediate; and *panel 3,* high level of mineralized fibers. *F,* calcium and phosphate concentrations in native and low (*panel 1*), intermediate (*panel 2*), and high (*panel 3*) levels of mineralized fibrils.

plaques showed bone-like regions with spatial distributions of minerals (51). In other studies, higher AGE levels in diabetes patients than in nondiabetic subjects were observed (52). Although several researchers have examined *in vitro* and *in vivo* mineralization and AGE accumulation of tissues in various diseases (22, 23, 53, 54), the consequences of such changes on the degradability of collagen macromolecules in affected or modified regions is unclear. In this study, we have used a combination of biochemical, ultrastructural, and cellular approaches to compare the degradation of modified collagen when exposed to CatK. Proteolytic degradation experiments indicate that mineralization prevents CatK-mediated hydrolysis of collagen fibers and fibrils. Our data indicate that intrafibrillar mineral deposits interfere with the CatK/collagen interactions during degradation, but in unmineralized collagen, CatK/collagen-binding sites remain readily accessible. Nudelman *et al.* (55) have previously shown that the mineral nucleation point is adjacent to the C terminus of tropocollagen molecules in the fibril (*i.e.* after the gap/overlap transition). A CatK/collagen interaction assay also showed a reduction in binding efficiency after mineralization when native and mineralized collagen fibers were compared. These data indicate that mineralization at the C termini may interfere with the binding of CatK to the initial cleavage sites (56), which are present in the same region (57), and thus explain the observed reduction in CTx release following digestion of mineralized collagen fibers.

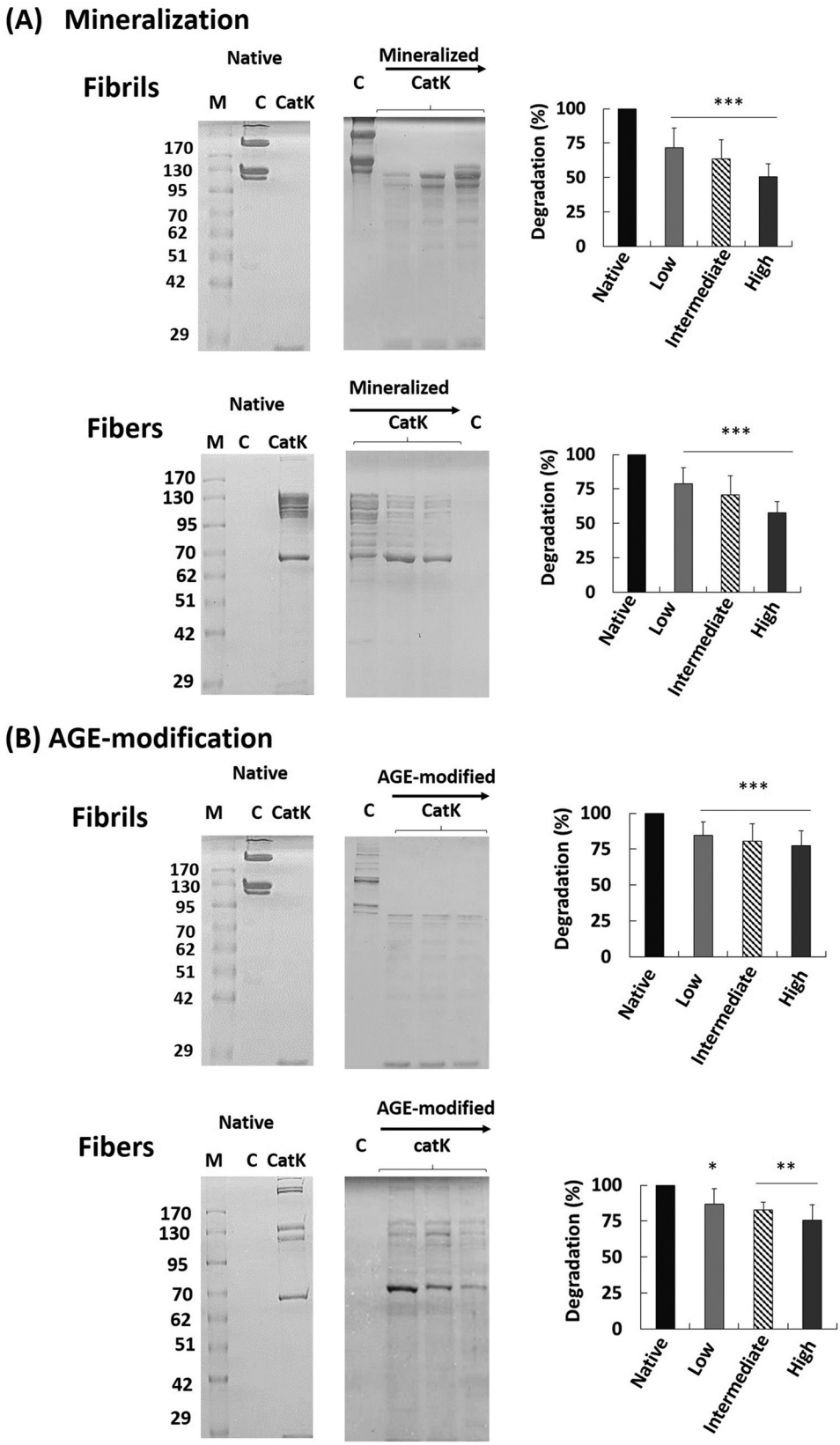

FIGURE 9. *A,* SDS-PAGE analyses show the comparative degradation of native and mineralized fibrils (*1st panel*) and fibers (*2nd panel*). Mineralized fibrils show less degradation with increasing mineral concentrations. Quantification of the degradation products of low, intermediate, and high degree of mineralized fibrils and fibers (*right side*). *Arrow* indicates increasing mineral content from low to high. *B,* SDS-PAGE analysis shows less degradation of AGE-modified collagen fibrils (*3rd panel*) and fibers (*4th panel*) compared with native collagen and their respective quantification (*right side*). *Arrow* indicates increasing AGE content from low to high. Increasing amounts of AGE displayed no significant effect on collagen fiber and fibril degradation. *M,* protein marker; *C,* control collagen without any modification. Statistical significance was tested with ANOVA. ***, $p < 0.001$; **, $p < 0.01$; and *, $p < 0.05$ *versus* native fibrils or fibers.

TABLE 3

Mechanical properties of native and differentially mineralized collagen fibers

MPa is megapascal and GPa is gigapascal.

Mineralization degree	Diameter	Strength	Young's modulus	Stress at break	Strain at break
	μm	*N*	*GPa*	*MPa*	*%*
Native	59.00 ± 14.81	2.02 ± 0.45	3.03 ± 0.40	605 ± 100	43 ± 6.9
Low	67.82 ± 13.74	2.81 ± 0.34	3.74 ± 0.25	713 ± 89	29 ± 4.2
Intermediate	72.55 ± 15.85	2.94 ± 0.52	3.90 ± 0.50	740 ± 77	26 ± 3.1
High	77.43 ± 11.63	3.01 ± 0.63	3.95 ± 0.47	781 ± 98	22 ± 5.3

TABLE 4

Mechanical properties of native and AGE-modified collagen fibers

MPa is megapascal and GPa is gigapascal.

Fiber treatment	Diameter	Strength	Young's modulus	Stress at break	Strain at break
	μm	*N*	*GPa*	*MPa*	*%*
Native	59.00 ± 14.81	2.02 ± 0.45	3.03 ± 0.40	605 ± 100	43 ± 6.9
AGEs (low)	74.64 ± 12.71	2.47 ± 0.56	3.48 ± 0.27	688 ± 75	36 ± 4.8
AGEs (high)	81.63 ± 10.41	2.68 ± 0.33	3.72 ± 0.47	706 ± 103	31 ± 6.2

The effect of mineralization on the mechanical properties of tissues has been intensively studied (58, 59). The combined distribution of stress and strain by minerals and collagen provides unique mechanical properties to the skeleton (60, 61). However, in the vascular system, cartilage, and soft tissues, excessive stiffness of collagenous components by mineralization may cause severe complications (19, 53). Using different approaches, we assessed the mechanical properties of collagen macromolecules at distinct hierarchical levels. There is direct evidence from AFM analysis that an increase in the mineral content changes stiffness of fibrils. Mineralized fibrils exhibit the highest moduli compared with native fibrils. Consistent with these results, the elastic moduli of normal and mineralized mature fibrils was recently found to be in this range under tensile loading using different techniques (6, 61). Altogether, our study indicates that mineralization of collagen at both fiber and fibril levels reduces their intrinsic flexibility, which is an asset in bones. However, this is a drawback in arteries and other soft tissues, where excessive stiffness reduces the functionality of the tissue and leads to a range of disorders (19, 20). Appreciable concentrations of calcium, phosphorus, silicium, and sulfur in the calcified lesions of spherical forms have been reported previously (51, 62). It can be assumed that the degree of mineralization at these foci is comparable with our *in vitro* mineralized collagen fibers.

Although collagen cross-linking is necessary to stabilize fibrils and provides elasticity and mechanical strength to the tissue, excessive cross-links formed in collagen during aging and diseases may compromise the biomechanical integrity of tissues (63, 64). An increase in stiffness and reduction in elasticity of tissues due to AGEs during aging has been reported previously (65, 66). Here, we examined the effects of AGE modification on collagen and compared the changes in collagen structure and degradability. On the basis of these observations, it can be stated that accumulation of AGEs in collagen fibers reduces their degradation by CatK. Changes from native to AGE-modified conditions caused a drop in the maximal stretching and a slight increase in the modulus of fibers. Moreover, at the nanostructural level, AFM results confirmed that fibril stiffness increased with AGE accumulation and is in agreement with a previous study (67).

In addition to collagen, PGs and other glycoproteins play an important role in maintaining the biomechanical properties of the matrix. GAG-carrying PGs are hydrophilic molecules responsible for the hydration and load-bearing mechanism of the tissue (68). Alteration of GAGs in tissues during aging has been demonstrated in many studies (69, 70). Our earlier studies have shown that GAGs are required for CatK-mediated collagen degradation. GAGs are needed to form oligomeric CatK complexes, which act as collagenases (71). The results of this study clearly indicate that GAG-depleted fibers are resistant to CatK digestion as they revealed no changes in the organization of fibers and fibrils after incubation with the protease. We have shown that GAGs facilitate the binding of CatK to collagen fibers (56). GAG-deficient fibers displayed minimum Young's moduli. No significant changes were observed after CatK digestion in the mechanical properties of GAG-depleted fibers. Based on the qualitative images, mechanical data, and quantitative degradation information, a schematic representation of the action of CatK-mediated collagen degradation is depicted in Scheme 1.

Besides matrix metalloproteases (72), CatK is crucial in ECM remodeling. Matrix degradation is essential to replace damaged and modified proteins, to allow for the regeneration of tissues, and to maintain their normal structure and function (26, 27, 29, 73). During physiological conditions, type I collagen in soft tissues has a faster turnover than in bone because of its lower degree of isomerization and deoxypyridinoline cross-links (74). This study indicates that CatK-mediated degradation of type I collagen is reduced following mineralization, AGE accumulation, and other modifications. However, OC-mediated collagen turnover is increased in aged bones, which is likely to be an attempt to repair damaged bones, but it may also lead to an increased risk of osteoporosis. This highlights the differences between collagen digestion in aged tissues and bone matrix. The cellular environment may play a significant role in the different responses to age modification in different tissues. Whereas in soft tissues, macrophages, smooth muscle cells, and

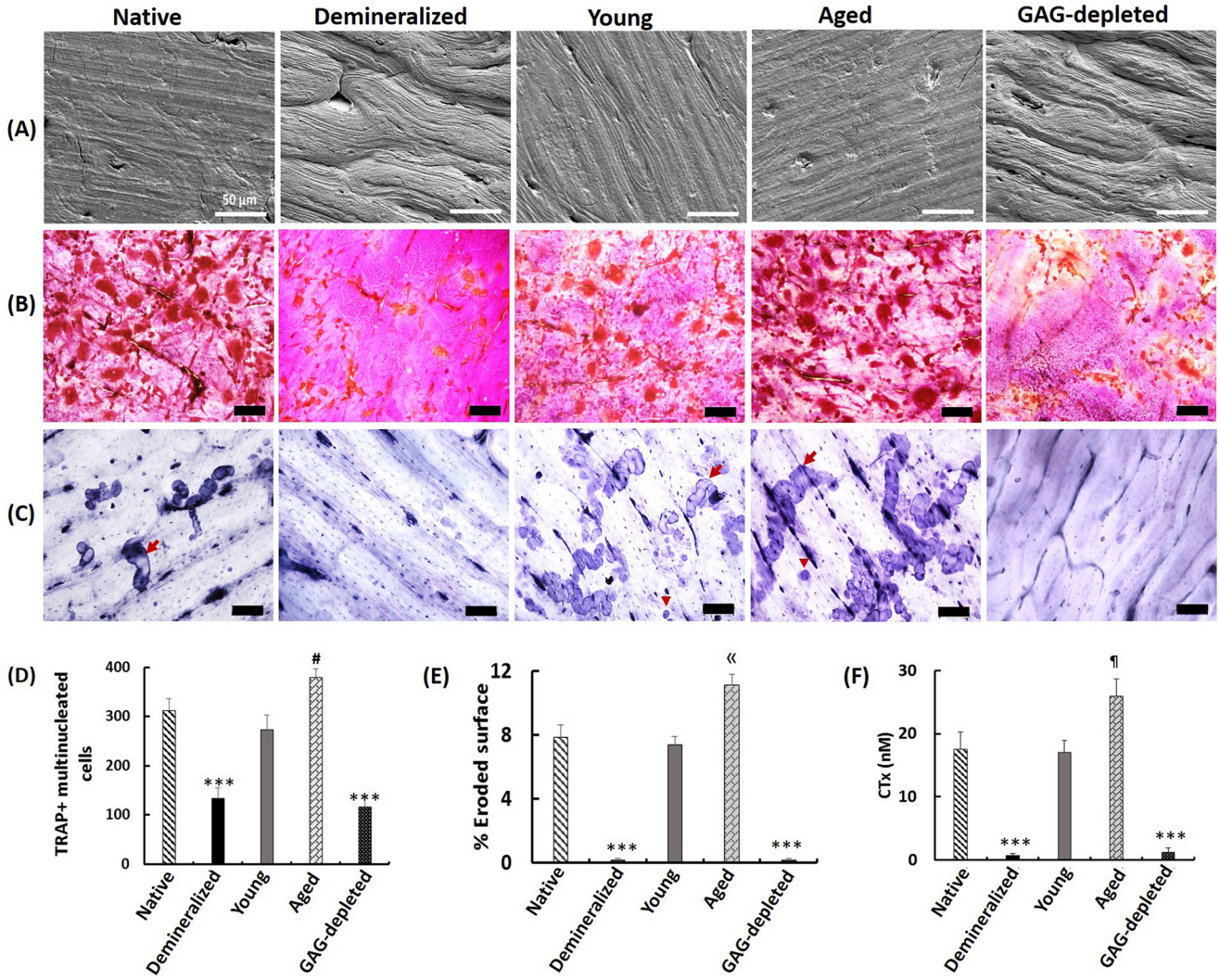

FIGURE 10. *A,* scanning electron micrograph of the surface of native, young, aged, demineralized, and GAG-depleted bone slices. *Scale bar,* 50 μm. *B,* images of TRAP-positive multinucleated osteoclasts cultured for 72 h on native, demineralized, young, aged, and GAG-depleted bone slices showing the adhesion rate of osteoclasts. *C,* representative images of resorption lacunae generated by OCs in respective conditions. *Scale bar,* 20 μm. Resorption cavities generated by OCs are in the form of trenches (*arrows*) and pits (*arrowheads*). *D,* effect of bone modification on number of multinucleated cells in terms of attachment at the bone surface. *E,* percentage of resorbed or eroded surface per bone slice. *F,* release of CTx (marker of bone turnover) in culture medium in different conditions ($n = 3$). Statistical significance was tested with ANOVA. ***, $p < 0.001$ *versus* native bone; ≪, $p < 0.001$ *versus* young and native bone; #, $p < 0.01$ *versus* young and native bone; and ¶, $p < 0.05$ *versus* young bone.

TABLE 5

Mechanical properties of native and physiologically modified bone

MPa is megapascal.

Bone	Young's modulus	Ultimate strength	Strain at break
	MPa	*MPa*	*%*
Native	1015 ± 380	63 ± 14	2.2 ± 0.41
Demineralized	11 ± 4	3.8 ± 1.2	21.5 ± 4.67
Aged	1235 ± 316	45 ± 6	1.8 ± 0.25
Young	985 ± 393	59 ± 9	2.6 ± 0.53

fibroblasts express CatK in response to stresses and internalize fragments of the ECM (29, 75), CatK-expressing OCs migrate to damaged bone and degrade it (76). In this context, a complete inhibition of CatK in elderly patients suffering from osteoporosis may indiscriminately block necessary collagen turnover outside of the skeletal system. This might be of concern with regard to the high potency of CatK inhibitors currently developed as a therapeutic agent for the treatment of osteoporosis (30, 32). Although beneficial in bone, a significant inhibition of CatK-mediated tissue remodeling in other tissues may increase the risk of disorders within the ECM. As shown in this report, aging-related modifications of collagen disturb normal proteolytic hydrolysis, and this may be exacerbated by current strategies to inhibit CatK in elderly patients. To avoid the total inhibition of CatK, strategies must be developed to specifically target the diseased areas using specific drug delivery methods.

Conclusions

Our results indicate that aging-associated collagen modifications disturb mechanical properties, disrupt physiologically essential CatK-mediated remodeling of collagen, and are thus critical in the progression of ECM pathologies. These modifications reflect differentiality in soft tissues and the skeletal system. High elastic moduli, low deformation, and reduced proteolytic degradation of fibrils and fibers following mineralization and AGE accumulation indicate an increased risk of

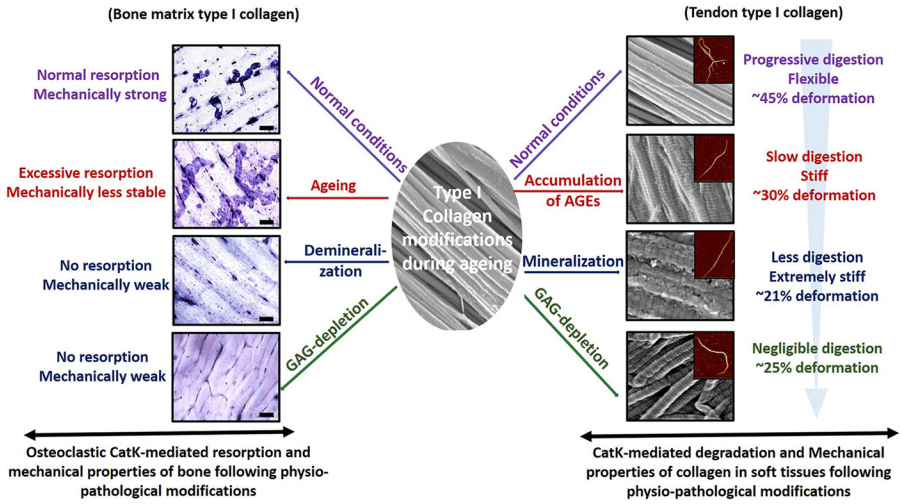

SCHEME 1. **Schematic presentation of the impact of physiological modifications on the structural-mechanical properties and degradability of native and modified collagen in bone matrix and soft tissues.**

soft tissue disorders with age. On the contrary, excessive OC-mediated bone resorption in aged bones is a clear sign of osteoporosis. On the contrary, excessive OC-mediated bone resorption occurs in aged bones leading to osteoporosis. Therefore, selective approaches must be developed that allow tissue-specific collagen remodeling. It should be noted that *in vitro* studies have their limitations. Under *in vivo* conditions, additional factors such as mineralization enhancer and inhibitors contribute to the mineralization process, and the elemental composition and concentration may vary within a tissue and from one tissue type to another. Therefore, further studies are required to consolidate these conditions within an *in vivo* disease model.

Author Contributions—D. B. and P. P. designed the research; P. P. performed the research with G. L., N. C. W. M., and H. Y. P. P., G. L., F. K., H. L., and D. B. analyzed the data. P. P. and D. B. wrote the paper. All authors reviewed the results and approved the final version of the manuscript.

Acknowledgments—We are grateful to Centre for High-Throughput Phenogenomics at The University of British Columbia, particularly Dr. Gethin Owen for technical support in microscopy. We are thankful to Louis Choi for assistance in mechanical testing of collagen fibers. We also thank Dr. Ricardo Carvalho for help in the preparation of bone slices and Ingrid Ellis for editorial assistance in the final preparation of the manuscript.

References

1. Fratzl, P. (ed) (2008) Collagen: Structure and Mechanics, pp. 1–505. Springer Science and Business Media, LLC, New York
2. Engel, J., and Bächinger, H. P. (2005) Structure, stability and folding of the collagen triple helix. *Top. Curr. Chem.* **247,** 7–33
3. Orgel, J. P., Irving, T. C., Miller, A., and Wess, T. J. (2006) Microfibrillar structure of type I collagen *in situ*. *Proc. Natl. Acad. Sci. U.S.A.* **103,** 9001–9005
4. Zhang, G., Ezura, Y., Chervoneva, I., Robinson, P. S., Beason, D. P., Carine, E. T., Soslowsky, L. J., Iozzo, R. V., and Birk, D. E. (2006) Decorin regulates assembly of collagen fibrils and acquisition of biomechanical properties during tendon development. *J. Cell Biochem.* **98,** 1436–1449
5. Kalamajski, S., and Oldberg, A. (2010) The role of small leucine-rich proteoglycans in collagen fibrillogenesis. *Matrix Biol.* **29,** 248–253
6. Gautieri, A., Vesentini, S., Redaelli, A., and Buehler, M. J. (2011) Hierarchical structure and nanomechanics of collagen microfibrils from the atomistic scale up. *Nano. Lett.* **11,** 757–766
7. Connizzo, B. K., Sarver, J. J., Birk, D. E., Soslowsky, L. J., and Iozzo, R. V (2013) Effect of age and proteoglycan deficiency on collagen fiber re-alignment and mechanical properties in mouse supraspinatus tendon. *J. Biomech. Eng.* **135,** 021019
8. Ameye, L., and Young, M. F. (2002) Mice deficient in small leucine-rich proteoglycans: novel *in vivo* models for osteoporosis, osteoarthritis, Ehlers-Danlos syndrome, muscular dystrophy, and corneal diseases. *Glycobiology* **12,** 107–116
9. Cavalcante, F. S., Ito, S., Brewer, K., Sakai, H., Alencar, A. M., Almeida, M. P., Andrade, J. S., Jr., Majumdar, A., Ingenito, E. P., and Suki, B. (2005) Mechanical interactions between collagen and proteoglycans: implications for the stability of lung tissue. *J. Appl. Physiol.* **98,** 672–679
10. Mays, P. K., McAnulty, R. J., Campa, J. S., and Laurent, G. J. (1991) Age-related changes in collagen synthesis and degradation in rat tissues. Importance of degradation of newly synthesized collagen in regulating collagen production. *Biochem. J.* **276,** 307–313
11. Rolewska, P., Al-Robaiy, S., Navarrete Santos, A., Simm, A., Silber, R.-E., and Bartling, B. (2013) Age-related expression, enzymatic solubility and modification with advanced glycation end products of fibrillar collagens in mouse lung. *Exp. Gerontol.* **48,** 29–37
12. Varani, J., Dame, M. K., Rittie, L., Fligiel, S. E., Kang, S., Fisher, G. J., and Voorhees, J. J. (2006) Decreased collagen production in chronologically aged skin: roles of age-dependent alteration in fibroblast function and defective mechanical stimulation. *Am. J. Pathol.* **168,** 1861–1868
13. Hofbauer, L. C., Brueck, C. C., Shanahan, C. M., Schoppet, M., and Dobnig, H. (2007) Vascular calcification and osteoporosis–from clinical observation towards molecular understanding. *Osteoporos Int.* **18,** 251–259
14. Tang, S. Y., and Vashishth, D. (2011) The relative contributions of non-enzymatic glycation and cortical porosity on the fracture toughness of aging bone. *J. Biomech.* **44,** 330–336
15. Sell, D. R., and Monnier, V. M. (2012) Molecular basis of arterial stiffening: role of glycation–a mini-review. *Gerontology* **58,** 227–237
16. Verzijl, N., DeGroot, J., Ben, Z. C., Brau-Benjamin, O., Maroudas, A., Bank, R. A., Mizrahi, J., Schalkwijk, C. G., Thorpe, S. R., Baynes, J. W., Bijlsma, J. W., Lafeber, F. P., and TeKoppele, J. M. (2002) Crosslinking by advanced glycation end products increases the stiffness of the collagen network in human articular cartilage: a possible mechanism through which age is a risk factor for osteoarthritis. *Arthritis Rheum.* **46,** 114–123
17. Verzijl, N., DeGroot, J., Thorpe, S. R., Bank, R. A., Shaw, J. N., Lyons, T. J., Bijlsma, J. W., Lafeber, F. P., Baynes, J. W., and TeKoppele, J. M. (2000) Effect of collagen turnover on the accumulation of advanced glycation end products. *J. Biol. Chem.* **275,** 39027–39031

18. Fuerst, M., Bertrand, J., Lammers, L., Dreier, R., Echtermeyer, F., Nitschke, Y., Rutsch, F., Schäfer, F. K., Niggemeyer, O., Steinhagen, J., Lohmann, C. H., Pap, T., and Rüther, W. (2009) Calcification of articular cartilage in human osteoarthritis. *Arthritis Rheum.* **60,** 2694–2703
19. Johnson, R. C., Leopold, J. A., and Loscalzo, J. (2006) Vascular calcification: pathobiological mechanisms and clinical implications. *Circ. Res.* **99,** 1044–1059
20. Rodriguez, K. J., Piechura, L. M., Porras, A. M., and Masters, K. S. (2014) Manipulation of valve composition to elucidate the role of collagen in aortic valve calcification. *BMC Cardiovasc. Disord.* **14,** 29
21. Martin, K. J., and González, E. A. (2007) Metabolic bone disease in chronic kidney disease. *J. Am. Soc. Nephrol.* **18,** 875–885
22. Basta, G., Schmidt, A. M., and De Caterina, R. (2004) Advanced glycation end products and vascular inflammation: implications for accelerated atherosclerosis in diabetes. *Cardiovasc. Res.* **63,** 582–592
23. Noordzij, M. J., Lefrandt, J. D., and Smit, A. J. (2008) Advanced glycation end products in renal failure: an overview. *J. Ren. Care* **34,** 207–212
24. Avery, N. C., and Bailey, A. J. (2006) The effects of the Maillard reaction on the physical properties and cell interactions of collagen. *Pathol. Biol.* **54,** 387–395
25. Garnero, P. (2012) The contribution of collagen crosslinks to bone strength. *Bonekey Rep.* **1,** 182
26. Cox, T. R., and Erler, J. T. (2011) Remodeling and homeostasis of the extracellular matrix: implications for fibrotic diseases and cancer. *Dis. Models Mech.* **4,** 165–178
27. Lu, P., Takai, K., Weaver, V. M., and Werb, Z. (2011) Extracellular matrix degradation and remodeling in development and disease. *Cold Spring Harb. Perspect. Biol.* **3,** a005058
28. Everts, V., Korper, W., Hoeben, K. A., Jansen, I. D., Bromme, D., Cleutjens, K. B., Heeneman, S., Peters, C., Reinheckel, T., Saftig, P., and Beertsen, W. (2006) Osteoclastic bone degradation and the role of different cysteine proteinases and matrix metalloproteinases: differences between calvaria and long bone. *J. Bone Miner. Res.* **21,** 1399–1408
29. Hu, L., Cheng, X. W., Song, H., Inoue, A., Jiang, H., Li, X., Shi, G.-P., Kozawa, E., Okumura, K., and Kuzuya, M. (2014) Cathepsin K activity controls injury-related vascular repair in mice. *Hypertension* **63,** 607–615
30. Cheng, X. W., Huang, Z., Kuzuya, M., Okumura, K., and Murohara, T. (2011) Cysteine protease cathepsins in atherosclerosis-based vascular disease and its complications. *Hypertension* **58,** 978–986
31. Cheng, X. W., Kikuchi, R., Ishii, H., Yoshikawa, D., Hu, L., Takahashi, R., Shibata, R., Ikeda, N., Kuzuya, M., Okumura, K., and Murohara, T. (2013) Circulating cathepsin K as a potential novel biomarker of coronary artery disease. *Atherosclerosis* **228,** 211–216
32. Duong, L. T. (2013) Inhibition of cathepsin K: blocking osteoclast bone resorption and more. *IBMS Bonekey.* 10.1038/bonekey.2013.130
33. Papazafiropoulou, A., and Tentolouris, N. (2009) Matrix metalloproteinases and cardiovascular diseases. *Hippokratia* **13,** 76–82
34. Malemud, C. J. (2006) Matrix metalloproteinases (MMPs) in health and disease: an overview. *Front. Biosci.* **11,** 1696–1701
35. Linnevers, C. J., McGrath, M. E., Armstrong, R., Mistry, F. R., Barnes, M. G., Klaus, J. L., Palmer, J. T., Katz, B. A., and Brömme, D. (1997) Expression of human cathepsin K in *Pichia pastoris* and preliminary crystallographic studies of an inhibitor complex. *Protein Sci.* **6,** 919–921
36. Kokubo, T., and Takadama, H. (2006) How useful is SBF in predicting *in vivo* bone bioactivity? *Biomaterials* **27,** 2907–2915
37. Oyane, A., Kim, H.-M., Furuya, T., Kokubo, T., Miyazaki, T., and Nakamura, T. (2003) Preparation and assessment of revised simulated body fluids. *J. Biomed. Mater. Res. A* **65,** 188–195
38. Monnier, V. M., Kohn, R. R., and Cerami, A. (1984) Accelerated age-related browning of human collagen in diabetes mellitus. *Proc. Natl. Acad. Sci. U.S.A.* **81,** 583–587
39. Farndale, R. W., Sayers, C. A., and Barrett, A. J. (1982) A direct spectrophotometric microassay for sulfated glycosaminoglycans in cartilage cultures. *Connect. Tissue Res.* **9,** 247–248
40. Lamour, G., Yip, C. K., Li, H., and Gsponer, J. (2014) High intrinsic mechanical flexibility of mouse prion nanofibrils revealed by measurements of axial and radial Young's moduli. *ACS Nano* **8,** 3851–3861
41. Lamour, G., Kirkegaard, J. B., Li, H., Knowles, T. P., and Gsponer, J. (2014) Easyworm: an open-source software tool to determine the mechanical properties of worm-like chains. *Source Code Biol. Med.* **9,** 16
42. Knowles, T. P., Fitzpatrick, A. W., Meehan, S., Mott, H. R., Vendruscolo, M., Dobson, C. M., and Welland, M. E. (2007) Role of intermolecular forces in defining material properties of protein nanofibrils. *Science* **318,** 1900–1903
43. Valle, F., Favre, M., De Los Rios, P., Rosa, A., and Dietler, G. (2005) Scaling exponents and probability distributions of DNA end-to-end distance. *Phys. Rev. Lett.* **95,** 158105
44. Panwar, P., Du, X., Sharma, V., Lamour, G., Castro, M., Li, H., and Brömme, D. (2013) Effects of cysteine proteases on the structural and mechanical properties of collagen fibers. *J. Biol. Chem.* **288,** 5940–5950
45. Tan, E. P., Ng, S. Y., and Lim, C. T. (2005) Tensile testing of a single ultrafine polymeric fiber. *Biomaterials* **26,** 1453–1456
46. Søe, K., and Delaissé, J.-M. (2010) Glucocorticoids maintain human osteoclasts in the active mode of their resorption cycle. *J. Bone Miner. Res.* **25,** 2184–2192
47. Smith, J. F., Knowles, T. P., Dobson, C. M., Macphee, C. E., and Welland, M. E. (2006) Characterization of the nanoscale properties of individual amyloid fibrils. *Proc. Natl. Acad. Sci. U.S.A.* **103,** 15806–15811
48. Knowles, T. P., Smith, J. F., Craig, A., Dobson, C. M., and Welland, M. E. (2006) Spatial persistence of angular correlations in amyloid fibrils. *Phys. Rev. Lett.* **96,** 238301
49. Schmid, K., McSharry, W. O., Pameijer, C. H., and Binette, J. P. (1980) Chemical and physicochemical studies on the mineral deposits of the human atherosclerotic aorta. *Atherosclerosis* **37,** 199–210
50. Olsson, L. F., Odselius, R., Ribbe, E., and Hegbrant, J. (2001) Evidence of calcium phosphate depositions in stenotic arteriovenous fistulas. *Am. J. Kidney Dis.* **38,** 377–383
51. Bertazzo, S., Gentleman, E., Cloyd, K. L., Chester, A. H., Yacoub, M. H., and Stevens, M. M. (2013) Nano-analytical electron microscopy reveals fundamental insights into human cardiovascular tissue calcification. *Nat. Mater.* **12,** 576–583
52. Huebschmann, A. G., Regensteiner, J. G., Vlassara, H., and Reusch, J. E. (2006) Diabetes and advanced glycoxidation end products. *Diabetes Care* **29,** 1420–1432
53. Demer, L. L., and Tintut, Y. (2008) Vascular calcification: pathobiology of a multifaceted disease. *Circulation* **117,** 2938–2948
54. Stirban, A., Gawlowski, T., and Roden, M. (2014) Vascular effects of advanced glycation end products: Clinical effects and molecular mechanisms. *Mol. Metab.* **3,** 94–108
55. Nudelman, F., Pieterse, K., George, A., Bomans, P. H., Friedrich, H., Brylka, L. J., Hilbers, P. A., de With, G., and Sommerdijk, N. A. (2010) The role of collagen in bone apatite formation in the presence of hydroxyapatite nucleation inhibitors. *Nat. Mater.* **9,** 1004–1009
56. Aguda, A. H., Panwar, P., Du, X., Nguyen, N. T., Brayer, G. D., and Brömme, D. (2014) Structural basis of collagen fiber degradation by cathepsin K. *Proc. Natl. Acad. Sci. U.S.A.* **111,** 17474–17479
57. Wheater, G., Elshahaly, M., Tuck, S. P., Datta, H. K., and van Laar, J. M. (2013) The clinical utility of bone marker measurements in osteoporosis. *J. Transl. Med.* **11,** 201
58. Ebenstein, D. M., Coughlin, D., Chapman, J., Li, C., and Pruitt, L. A. (2009) Nanomechanical properties of calcification, fibrous tissue, and hematoma from atherosclerotic plaques. *J. Biomed. Mater. Res. A* **91,** 1028–1037
59. Ferguson, V. L., Bushby, A. J., and Boyde, A. (2003) Nanomechanical properties and mineral concentration in articular calcified cartilage and subchondral bone. *J. Anat.* **203,** 191–202
60. Koester, K. J., Ager, J. W., 3rd, and Ritchie, R. O. (2008) The true toughness of human cortical bone measured with realistically short cracks. *Nat. Mater.* **7,** 672–677
61. Nair, A. K., Gautieri, A., Chang, S.-W., and Buehler, M. J. (2013) Molecular mechanics of mineralized collagen fibrils in bone. *Nat. Commun.* **4,** 1724
62. Thiam, S., Tracy, R. E., Robinson, J. W., and Warner, I. M. (2004) Determination of elements in native and bypass human coronary artery plaque deposits from the same heart using inductively coupled plasma-mass spectrometry. *J. Environ. Sci. Health. A Tox. Hazard Subst. Environ. Eng.* **39,** 1497–1503
63. Goh, K. L., Holmes, D. F., Lu, H.-Y., Richardson, S., Kadler, K. E., Purslow,

P. P., and Wess, T. J. (2008) Ageing changes in the tensile properties of tendons: influence of collagen fibril volume fraction. *J. Biomech. Eng.* **130,** 021011
64. Ebrahimi, A. P. (2009) Mechanical properties of normal and diseased cerebrovascular system. *J. Vasc. Interv. Neurol.* **2,** 155–162
65. Reddy, G. K. (2004) AGE-related cross-linking of collagen is associated with aortic wall matrix stiffness in the pathogenesis of drug-induced diabetes in rats. *Microvasc. Res.* **68,** 132–142
66. Haus, J. M., Carrithers, J. A., Trappe, S. W., and Trappe, T. A. (2007) Collagen, cross-linking, and advanced glycation end products in aging human skeletal muscle. *J. Appl. Physiol.* **103,** 2068–2076
67. Buehler, M. J. (2008) Nanomechanics of collagen fibrils under varying cross-link densities: atomistic and continuum studies. *J. Mech. Behav. Biomed. Mater.* **1,** 59–67
68. Yanagishita, M. (1993) Function of proteoglycans in the extracellular matrix. *Acta Pathol. Jpn.* **43,** 283–293
69. Li, Y., Liu, Y., Xia, W., Lei, D., Voorhees, J. J., and Fisher, G. J. (2013) Age-dependent alterations of decorin glycosaminoglycans in human skin. *Sci. Rep.* **3,** 2422
70. Ernst, S., Langer, R., Cooney, C. L., and Sasisekharan, R. (1995) Enzymatic degradation of glycosaminoglycans. *Crit. Rev. Biochem. Mol. Biol.* **30,** 387–444
71. Li, Z., Hou, W.-S., Escalante-Torres, C. R., Gelb, B. D., and Bromme, D. (2002) Collagenase activity of cathepsin K depends on complex formation with chondroitin sulfate. *J. Biol. Chem.* **277,** 28669–28676
72. Paiva, K. B., and Granjeiro, J. M. (2014) Bone tissue remodeling and development: focus on matrix metalloproteinase functions. *Arch. Biochem. Biophys.* **561,** 74–87
73. Lutgens, S. P., Cleutjens, K. B., Daemen, M. J., and Heeneman, S. (2007) Cathepsin cysteine proteases in cardiovascular disease. *FASEB J.* **21,** 3029–3041
74. Gineyts, E., Cloos, P. A., Borel, O., Grimaud, L., Delmas, P. D., and Garnero, P. (2000) Racemization and isomerization of type I collagen C-telopeptides in human bone and soft tissues: assessment of tissue turnover. *Biochem. J.* **345,** 481–485
75. Jaffer, F. A., Kim, D.-E., Quinti, L., Tung, C.-H., Aikawa, E., Pande, A. N., Kohler, R. H., Shi, G.-P., Libby, P., and Weissleder, R. (2007) Optical visualization of cathepsin K activity in atherosclerosis with a novel, protease-activatable fluorescence sensor. *Circulation* **115,** 2292–2298
76. Crockett, J. C., Rogers, M. J., Coxon, F. P., Hocking, L. J., and Helfrich, M. H. (2011) Bone remodelling at a glance. *J. Cell Sci.* **124,** 991–998